Journal of Materials Chemistry B

Accepted Manuscript

ROYAL SOCIETY OF CHEMISTRY

www.rsc.org/materialsB

In situ synthesis, characterization and *in vitro* studies of ciprofloxacin loaded hydroxyapatite nanoparticles for the treatment of osteomyelitis

G. Suresh Kumar, R. Govindan and E.K. Girija*

Department of Physics, Periyar University, Salem 636 011, India

** Corresponding author. Tel: + 91 9444391733, Fax: +91 427 2345124.*

E-mail address: girijaeaswaradas@gmail.com (E.K. Girija).

Abstract

Bioactive materials in combination with antibiotics are widely developed for the treatment of osteomyelitis which play a dual role: as bone substitute at the affected site and as local drug delivery system for an antibiotic delivery. In the present study, a series of ciprofloxacin loaded hydroxyapatite (HA) nanoparticles with sustained and prolonged release behavior has been synthesized by *in situ* precipitation method. The amount of ciprofloxacin loaded on HA nanoparticles can be easily adjusted by changing the initial concentration during the synthesis. It was observed that as the loaded concentration of ciprofloxacin increases the release is sustained and prolonged. The *in situ* loading of ciprofloxacin onto HA nanoparticles does not significantly affect the bioactivity and cytocompatibility of HA whereas it provides antibacterial activity to HA against *S. aureus* and *E. coli* that causes osteomyelitis. Consequently synthesized ciprofloxacin loaded HA nanoparticles can be a potential candidate for the treatment of osteomyelitis.

Keywords: Hydroxyapatite; *In situ* synthesis; Bioactivity; Drug delivery; Osteomyelitis;

1. Introduction

Osteomyelitis is an inflammation of bone caused by infective micro-organisms [1-3]. The usual treatment of osteomyelitis mainly involves fundamental surgical debridement of the infected bone, filling the bone defect, adequate soft tissue coverage and antibiotic therapy. A prolonged course of antibiotic therapy is required, most often 4-6 weeks and sometimes longer [1-6]. Oral delivery of antibiotics can result in systemic toxicity associated with renal and liver complications and poor penetration into the targeted site [7-9]. Hence alternative strategy of antibiotic delivery should be explored. Recently, development of local drug delivery system received much attention since antibiotics are delivered locally, the side effects and risk of overdose of oral administration can be avoided and high concentration of drug can effectively reach the targeted site [7-11]. Bioactive materials in combination with antibiotics are very useful for the development of local drug delivery systems because they play a vital role in subsequent bone regeneration at the infected site [12, 13].

Hydroxyapatite (HA) is one of the well known biomaterials owing to its high biocompatibility, bioactivity and osteoconductivity, also it is the main mineral component of bones and teeth [14]. Mostly HA exists in hexagonal crystal structure and offer two different binding sites such as positively charged Ca sites and negatively charged P sites on its surface [15]. Thus, HA surface has high adsorption ability for many substances such as proteins, antibiotics and growth factors [15-29]. Usually drug loading on HA was achieved either via simple adsorption process [17-20] or by solid state mixing of drug with HA powder [22, 23]. The earlier mode can result in limited drug loading efficiency and burst release behavior whereas the later one can result in the heterogeneous drug distribution within HA matrix and uncontrolled release behavior. Hence, search for alternative drug loading modality to achieve sustained and prolonged drug release has lead to the option of *in situ* drug loading [24-26].

There are several antibiotics extensively studied for the treatment of osteomyelitis [2]. Among the several antibiotics, ciprofloxacin is much preferred for the treatment of osteomyelitis since its minimal inhibitory concentration (MIC) is low (0.25–2 μg/ml) for most of the pathogens that cause osteomyelitis [27-29]. Aim of the present work is to synthesize HA nanoparticles having the potential to deliver ciprofloxacin in a sustained and prolonged manner.

2. Experimental procedure

2.1. *In situ* synthesis of ciprofloxacin loaded HA nanoparticles

Analytical grade calcium nitrate tetrahydrate ($Ca(NO_3)_2 \cdot 4H_2O$), di-ammonium hydrogen phosphate ($(NH_4)_2HPO_4$) and ammonia solution (NH_4OH) were purchased from Merck, India. Ciprofloxacin hydrochloride monohydrate ($C_{17}H_{18}FN_3O_3.HCl.H_2O$) was purchased from Himedia, India. All chemicals were used without further purification. Deionized water was employed as the solvent.

Ciprofloxacin loaded HA nanoparticles were prepared by an *in situ* precipitation method. Briefly, appropriate amount of $Ca(NO_3)_2 \cdot 4H_2O$ (1M), $(NH_4)_2HPO_4$ (0.6M) and $C_{17}H_{18}FN_3O_3.HCl.H_2O$ solutions were separately brought to pH = 10 with 25% NH_4OH. Then $(NH_4)_2HPO_4$ and $C_{17}H_{18}FN_3O_3.HCl.H_2O$ solutions were added dropwise into calcium nitrate solution under vigorous stirring at room temperature. The obtained reaction mixture was stirred for 1 h and aged for 24 h at room temperature. The reaction mixture was then centrifuged (5000 rpm) to separate the precipitate which was washed repeatedly to remove the byproducts. Then the precipitate was dried at 37 ºC and the dried cakes were crushed into powders. In order to load different amounts of $C_{17}H_{18}FN_3O_3.HCl.H_2O$ on HA nanoparticles, samples were prepared with 5, 10 and 20 mg/ml of $C_{17}H_{18}FN_3O_3.HCl.H_2O$ solutions and the samples obtained were named as HA-cip-1, HA-cip-2 and HA-cip-3, respectively. The same experiment was also carried out in the absence of $C_{17}H_{18}FN_3O_3.HCl.H_2O$ to obtain pure HA for comparison.

2.2. Characterization

The powder X-ray diffraction (PXRD) patterns of the as-synthesized samples were recorded using Rigaku MiniFlex II powder X-ray diffractometer in the range between $20° \leq 2\theta \leq 60°$ with Cu Kα monochromatic radiation (1.5406 Å). Crystallographic identification of the phases of the samples was accomplished by comparing the experimental PXRD pattern with standard data compiled by the International Center for Diffraction Data (ICDD). The average crystallite size was calculated from XRD data using the Scherrer approximation [30]

$$D_{hkl} = \frac{K\lambda}{\beta_{1/2}\cos\theta}$$

where D_{hkl} is the average crystallite size, as calculated for the (*hkl*) reflection, λ is the wavelength of Cu Kα radiation (1.5406 Å), $\beta_{1/2}$ is the full width at half maximum for the diffraction peak under consideration (in radian), θ is the diffraction angle (degree) and K is the broadening constant chosen as 0.9. The diffraction peak at 2θ = 25.8º was chosen for calculation of the crystallite size because it was sharper and isolated from others which is (002) Miller's plane of the HA crystal. The degree of crystallinity (*Xc*) was evaluated by using the following equation [31]

$$X_c = \left(\frac{0.24}{\beta_{002}} \right)^3$$

where β_{002} is the full width at half maximum (degree) of (002) Miller's plane. Fourier transform Infrared (FT-IR) spectra were recorded using BRUKER TENSOR 27 FT-IR spectrometer. The FT-IR spectra were recorded in the 4000–400 cm^{-1} region with 4 cm^{-1} resolution by using KBr pellet technique. The morphology of as-synthesized samples was examined using ZEISS ULTRA plus field emission scanning electron microscope (FESEM). The amount of ciprofloxacin present in as-synthesized samples were analyzed using thermogravimetry (TG) analyzer (Make:TA Instruments, Model: Q600).

2.3. *In vitro* studies

2.3.1. Bioactivity test

The bioactivity of the samples was studied by immersing the compacted samples in simulated body fluid (SBF) at 37 °C. The SBF was prepared by dissolving appropriate amount of reagent grade NaCl, $NaHCO_3$, KCl, Na_2HPO_4, $MgCl_2 \cdot 6H_2O$, Na_2SO_4, $(CH_2OH)_3CNH_2$ and $CaCl_2 \cdot 2H_2O$ in deionized water. 1M HCl was used to maintain pH of the solution at 7.4 to mimic the concentration of human blood plasma [32]. The as-synthesized samples were compacted into disk by applying a pressure of ~24 MPa. Then, the disk was immersed in 30 ml of SBF in plastic containers with airtight lids at 37 ± 0.5 °C in an incubator. The SBF solution was renewed once in three days for a period of three weeks. Finally, surface of the disk was analyzed by JEOL-6390 scanning electron microscope (SEM).

2.3.2. Cytocompatibility test

The cytocompatibility of HA and HA-cip-3 with human osteoblast like MG-63 cells was determined by the MTT assay [33]. The human osteoblast like MG-63 cells was purchased from National Centre for Cell Sciences (NCCS), Pune, India. For the MTT assay, the cells were grown in Eagles Minimum Essential Medium containing 10% fetal bovine serum (FBS) with 100 U/ml penicillin/streptomycin at 37 °C under a humidified atmosphere of 95% air and 5% CO_2. Maintained cultures were passaged every week and the culture medium was changed twice a week. The monolayer cells were detached with trypsin-ethylenediaminetetraacetic acid (EDTA) to make single cell suspensions and viable cells were counted using a hemocytometer and diluted with medium containing 5% FBS to give final density of $1x10^5$ cells/ml. 100 µl per well of cell suspension were seeded into 96-well plates at plating density of 10,000 cells/well and incubated at 37 °C in 5% CO_2, 95% air and 100% relative humidity. After 24 h incubation, samples HA and HA-cip-3 were added to the culture medium at different dosages (50, 100 and 200 µg/ml). The plates were further incubated for 48 h at 37 °C in 5% CO_2, 95% air and 100% relative humidity.

After 48 h incubation, 15 µl of 3-(4,5-dimethylthiazol-2-yl)-2,5-diphenyl tetrazolium bromide (MTT) solution (5 mg/ml in phosphate buffer saline (PBS)) was added into each well and the plate was further incubated for 4 h in the incubator. After discarding the supernatants, the dark blue formazan crystals were dissolved in 100 µl dimethyl sulfoxide (DMSO) and the optical density was measured using Synergy H4 microplate reader at 570 nm. The mean and the standard deviation were obtained from sums of three different experiments. Cell viability was calculated by using the following equation

$$\text{Cell viability (\%)} = (OD_{sample}/OD_{control}) \times 100$$

where OD_{sample} and $OD_{control}$ represent the optical density (OD) values of cells cultured with sample and without sample, respectively.

2.3.3. *In vitro* drug release study

To evaluate the *in vitro* release characteristics of ciprofloxacin hydrochloride from as-synthesized samples, 200 mg of as-synthesized samples were compacted into disk and then placed in a plastic container with 100 ml PBS of pH 7.4 at 37 ± 0.5 °C in incubator for appropriate time. The release medium was collected at various time intervals and the amount of

drug released was determined using a Perkin Elmer lambda 25 UV–vis spectrometer. The maximum absorbance wavelength (λ_{max}) for ciprofloxacin hydrochloride was found to be at 272 nm. The concentration of ciprofloxacin hydrochloride was calculated by employing a calibration curve. The experiments were repeated triplicate to get mean and the standard deviation.

2.3.4. Antibacterial activity

Antibacterial activity of all as-synthesized samples was studied by standard disc diffusion method [21]. As-synthesized samples were pressed at ~24 MPa to form disk, each nominally 8 mm diameter and 1 mm thick. The micro-organisms such as *Escherichia coli* (*E. coli*) and *Staphylococcus aureus* (*S. aureus*) were cultured on nutrient agar plates. After the culture, disks of samples were located on this plate and incubated for 24 h at 37 ± 0.5 °C. The microbial inhibition zone including disk was measured after the incubation period and its images were documented. The experiment was repeated three times in order to get mean and the standard deviation.

3. Results and discussions

3.1. Phase purity, morphology and TG analysis

The PXRD patterns of the as-synthesized samples are shown in Fig. 1. 2θ values of all the peaks observed in all samples matched well with JCPDS data for HA (JCPDS File No: 09-0432) which indicates that as-synthesized samples constitutes HA as a unique crystalline phase. The broad peak in the region 30-35° can be ascribed to (211), (112), (300) and (202) reflections of HA. The broadness of diffraction peaks slightly increased and the intensity decreased with increase in concentration of ciprofloxacin indicating the reduction in crystallite size and crystallinity. The calculated average crystallite size and degree of crystallinity of the as-synthesized samples from PXRD pattern are given in Table. 1. Significant reduction in crystallite size and crystallinity are observed for HA-cip-3.

FT-IR spectra of the as-synthesized samples are shown in Fig. 2. FT-IR spectrum of pure HA (Fig. 2 (a)) shows the characteristic PO_4^{3-} (υ_4) vibrations of HA at 565 and 602 cm^{-1} along with other υ_1, υ_2 and υ_3 phosphate peaks at 472, 961 and 1017-1109 cm^{-1} respectively. The bands at 3571 and 632 cm^{-1} are characteristic OH^- vibrations of HA [34-36]. The peaks present at 874,

1422 and 1455 cm^{-1} in the pure HA spectrum are attributed to the CO_3^{2-} ions, which is due to the adsorbed carbonate from atmosphere [36]. On the other hand, FT-IR spectrum of samples synthesized in the presence of ciprofloxacin (Fig. 2 (b-d)) showed the characteristic peaks of HA along with characteristic peaks of ciprofloxacin. A peak at 1627 cm^{-1} is assigned to C=O stretching vibrations of the carbonyl group [21, 37, 38]. The peaks at 1584 and 1384 cm^{-1} are due to antisymmetric ($\upsilon_{as}COO^-$) and symmetric (υ_sCOO^-) stretching vibrations of the carboxylic (COO^-) group, respectively [37-39]. The peak at 1272 cm^{-1} is attributed to C–F vibration of ciprofloxacin [21]. The peaks between 900–660 cm^{-1} are attributed to the C–H bending vibration of aromatic ring [21, 40]. The intensity of characteristic peaks of ciprofloxacin increased with increase in concentration of ciprofloxacin which indicate that more amount of ciprofloxacin is incorporated into HA when the concentration of ciprofloxacin was increased. Further, a strong band at 1632–1640 cm^{-1} and a broad band between 3000–3600 cm^{-1} observed in FT-IR spectrum of all samples may be attributed to the existence of adsorbed water in the samples [41].

FESEM images of as-synthesized samples are shown in Fig. 3. Pure HA consist of heavily aggregated nanometer sized particles. Whereas HA particles formed in the presence of ciprofloxacin are spherical in morphology and are loosely agglomerated. Particle size appears to increase with increase in concentration of ciprofloxacin.

TG curves of as-synthesized samples are shown in Fig. 4 (a). The weight loss observed upto 170 °C in all samples is due to desorption of physically adsorbed water molecules [42]. With increasing temperature, there is no significant weight loss for pure HA. On the other hand significant weight loss was observed between 170 and 600 °C for HA-cip-1, HA-cip-2 and HA-cip-3, due to the burning of ciprofloxacin [43]. From TG analysis, we have determined the amount of drug loaded on as-synthesized HA nanoparticles and the results are shown in Fig. 4 (b). It is found that the loading of ciprofloxacin on HA nanoparticles increased with increase of ciprofloxacin concentration. Moreover, the amount of ciprofloxacin loaded onto HA can be easily adjusted by changing the initial concentration of ciprofloxacin added during the synthesis of HA.

The obtained results from PXRD indicate that when the concentration of ciprofloxacin was increased, crystallite size decreased. Whereas FESEM analysis shows that particle size increased with increase in concentration of ciprofloxacin. Moreover FT-IR and TG analysis confirmed that ciprofloxacin content in as-synthesized samples increased with increase of the concentration of ciprofloxacin. A schematic illustrating the possible *in situ* formation of ciprofloxacin loaded HA nanoparticles is shown in Fig. 5. When calcium nitrate was added with di-ammonium hydrogen phosphate, the usual reaction between Ca and P takes place and result in the formation of amorphous calcium phosphate (ACP), which on aging leads to the development of HA crystallites (Fig. 5). On the other hand, the *in situ* presence of ciprofloxacin molecules during the formation of HA nanoparticles may lead to the strong interaction between carboxyl (COO^-) group of ciprofloxacin molecules and Ca^{2+} of ACP [26, 27]. Furthermore, F^- ions that are present in ciprofloxacin can also easily interact with HA on maturation [44]. Thus, due to the strong interaction between the ciprofloxacin molecules and HA nanoparticles more ciprofloxacin molecules may be incorporated into the interior of the HA nanoparticles in addition to the ciprofloxacin molecules adsorbed on the surface of the HA nanoparticles, as shown in Fig. 5. When the concentration of ciprofloxacin is increased more number of ciprofloxacin may interact with ACP and inhibit the crystallization of HA which resulted in the reduction of crystallite size and crystallinity. Whereas encapsulation of ciprofloxacin on HA crystallites due to adsorption increased with increase of concentration of ciprofloxacin and might have resulted in increased particle size.

3.2. In vitro studies

3.2.1. Bioactivity

Fig. 6 illustrates the SEM image of the surface of compacted samples (disk) before and after soaking in SBF for 21 days. SEM images before soaking in SBF showed the presence of micro-creaks on the surface whereas after soaking in SBF revealed the formation of apatite deposits on its surface. All the samples showed the formation of apatite deposits after immersion in SBF indicating that the bioactive nature of HA does not get affected by the incorporation of ciprofloxacin. The two different binding sites such as positively charged Ca sites and negatively charged P sites in HA surface can interact with negatively charged PO_4^{3-} and positively charged Ca^{2+} in SBF and result in the formation apatite deposits on the surface of compacted samples.

This bioactive nature represents the sign of *in vivo* bone bonding ability of as-synthesized samples. Formation of small dusts besides apatite deposits on HA-cip-1, HA-cip-2 and HA-cip-3 surfaces may be due to re-precipitation of ciprofloxacin molecules which is released during the immersion in SBF.

3.2.2. Cytocompatibility with human osteoblast like MG-63 cells

Fig. 7 shows the cell viability of human osteoblast like MG-63 cells cultured with HA and HA-cip-3 samples. Both samples showed good cell viability with human osteoblast like MG-63 cells since both sample contains HA which is main inorganic part of bones and teeth. Presence of ciprofloxacin molecules does not affect the cell viability of HA-cip-3. It is noted that the cell viability of both samples were decreased with increasing the dosage of the samples. Optical image of human osteoblast like MG-63 cells and cells cultured with different dosages of HA and HA-cip-3 are shown in Fig. 8 (a-g). According to biological evaluation of medical devices - Part 5: Tests for *in vitro* cytotoxicity (ISO 10993-5: 2009), if cell viability of material is less than 70 % then it has a cytotoxic potential [33]. However HA and HA-cip-3 exhibits cell viability greater than 93 % (Fig. 7) indicating that the as-synthesized samples are cytocompatible with human osteoblast like MG-63 cells.

3.2.3. In vitro drug release behavior

The amount of ciprofloxacin released from the *in situ* prepared ciprofloxacin loaded HA nanoparticles with time are shown in Fig. 9. HA-cip-2 and HA-cip-3 released relatively higher amount of ciprofloxacin than HA-cip-1. Whereas HA-cip-2 and HA-cip-3 exhibits similar release pattern upto 20 days, after that higher amount of ciprofloxacin was released from HA-cip-3 when compared with HA-cip-2. Moreover, rate of release at the initial stage (10 days) is higher and then it becomes gradual in all samples. Desorption of ciprofloxacin molecules that are located at the surface of the HA is responsible for higher initial release of ciprofloxacin whereas release of ciprofloxacin molecules from the interior of the HA nanoparticles by diffusion as well as dissolution processes is responsible for later release. It is interesting to note that the sustained and prolonged release of ciprofloxacin has been observed from all the samples. Fig. 10 shows the cumulative release percentage of ciprofloxacin from the *in situ* prepared ciprofloxacin loaded HA nanoparticles with time. Over the period of study 90% of the loaded ciprofloxacin was

successfully released from HA-cip-1 whereas only 65% and 32% of the loaded ciprofloxacin was released in HA-cip-2 and HA-cip-3, respectively. Significant quantities of ciprofloxacin molecules still remain in HA-cip-2 and HA-cip-3 and its can play an important role in prolonged antibiotic therapy for the treatment of osteomyelitis.

The drug release kinetics of the ciprofloxacin loaded HA nanoparticles were investigated using Higuchi model. It is well acknowledged that the Higuchi equation ($C = K_H t^{1/2}$) can very well describe the kinetics of the drug release from the carrier by a diffusion process through a linear relationship between the cumulative amount of released drug (C) and the square root of release time (t) [45, 46]. Fig. 11 shows a relationship between the cumulative amount of released drug and the square root of release time for the three drug delivery systems, which exhibited good linear relationship with a correlation coefficient (r^2) of 0.94 for HA-cip-1, 0.98 for HA-cip-2 and 0.99 for HA-cip-3 (Table 2). Hence drug release from the prepared drug delivery system is governed by diffusion process.

The drug release kinetics of the ciprofloxacin loaded HA nanoparticles were also investigated using Ritger-Peppas model. The Ritger-Peppas equation is $C = K_P t^n$, where C is the cumulative drug release at time t, K_P is a constant incorporating structural and geometric characteristics of the matrix and n is the diffusional exponent which indicates the drug release mechanism [47,48]. The drug release data were fitted into Ritger-Peppas model (Fig. 12), which exhibited good linear relationship between *log t* and *log C* and the kinetic parameters are summarized in Table 2. It is noted that the values of n are between 0.56 and 0.60 for all the samples which indicates that drug release from the prepared carriers are governed by anomalous (non-Fickian) diffusion mechanism [47, 48], which suggests the involvement of more than one process such as diffusion, surface erosion and desorption in the drug release mechanism [49, 50].

The performance of drug delivery devices mainly depends on the microstructure, degradation nature of the carrier, solubility of the drug and nature of the interactions between drug and carrier [51]. The *in situ* synthesis of samples can offer: (i) a strong interaction between Ca^{2+} of HA and COO^- group of ciprofloxacin [26, 27] and (ii) a strong interaction between of F^- ions in

ciprofloxacin molecules with HA on maturation [44] that resulted in sustained and prolonged release of ciprofloxacin from HA carriers.

3.2.4. Antibacterial activity against *E. coli* and *S. aureus*

S. aureus is the most common micro-organism found in patients of all kind of osteomyelitis whereas *E. coli* is commonly found in patients with chronic osteomyelitis [1, 3]. Antimicrobial activities of the as-synthesized samples against *E. coli* and *S. aureus* are shown in Fig. 13. There is no inhibition zone around pure HA. HA-cip-1, HA-cip-2 and HA-cip-3 showed inhibition zone around the pellet in which bacterial growth was inhibited. The diameter of inhibition zone of as-synthesized samples against *E. coli* and *S. aureus* are given in Table. 3. The observed antimicrobial activity of HA-cip-1, HA-cip-2 and HA-cip-3 can be due to the presence of ciprofloxacin molecules in the samples. Ciprofloxacin is a second generation fluoroquinolone antibiotic and it penetrate the bacterial cells and inhibit the enzymes such as DNA gyrase and topoisomerase IV, which are required for bacterial DNA replication and growth [52, 53]. The amount of drug release within 24 h from the fabricated drug delivery systems are well above the MIC of ciprofloxacin which is 0.25–2 μg/ml for most pathogens that causes osteomyelitis [27-29]. Hence HA-cip-1, HA-cip-2 and HA-cip-3 showed good antimicrobial activity against *E. coli* and *S. aureus*.

The clinical success of bone implants mainly depend on interfacial reaction between implants and surrounding tissues. Bone substitutes should ideally be bioactive, providing a chemical bond at the bone/implant interface [14, 54]. Bioactivity test revealed that all the synthesized samples have ability to form carbonated apatite layer on its surface in SBF and they may bond to living bone through the apatite layer formed on its surface in the living body. *In vitro* cellular test indicates that the prepared material does not contain a component that induces toxic effect. Moreover, a prolonged drug delivery system is required for the treatment of osteomyelitis and is achieved in the present study by *in situ* precipitation of ciprofloxacin with HA nanoparticles. Based on the above results, the prepared ciprofloxacin loaded HA nanoparticles can be considered as a potential candidate for the treatment of osteomyelitis since it can play dual role: as bone substitute at the affected site and as local drug delivery system for ciprofloxacin release.

Further *in vivo* studies are in progress to evaluate the effectiveness of ciprofloxacin loaded HA nanoparticles for the treatment of osteomyelitis.

4. Conclusions

A series of ciprofloxacin loaded HA nanoparticles with sustained and prolonged release behavior of ciprofloxacin were fabricated by *in situ* precipitation method. Tunable loading was achieved by changing the initial concentration of ciprofloxacin during synthesis. It is observed from the present study that as the concentration of ciprofloxacin is high, significant amount of ciprofloxacin molecules remain in HA carrier and plays a vital role in sustained and prolonged release. *In situ* incorporation of ciprofloxacin into HA does not significantly affect the bioactivity and cytocompatibility of HA whereas it provides antibacterial activity to HA against *S. aureus* and *E. coli* that causes osteomyelitis. Consequently the present study offers bone substitute material with the combined properties of HA and ciprofloxacin for the treatment of osteomyelitis.

Acknowledgments

This work was financially supported by University Grants Commission, India through project (Project Ref. No.: 41-1013/2012 SR). One of the authors G. Suresh Kumar acknowledges the Council of Scientific and Industrial Research, India for the award of Senior Research Fellowship (File No.: 09/810(0016)/2012- EMR-I). The discussions with Dr. A. Thamizhavel, Department of Condensed Matter Physics and Materials Science, Tata Institute of Fundamental Research, India are gratefully acknowledged.

References

[1] P. J. Carek, L. M. Dickerson and J. L. Sack, *Am. Fam. Physician.,* 2001, **63,** 2413-2420.

[2] S. K. Nandi, P. Mukherjee, S. Roy, B. Kundu, D. K. De and D. Basu, *Mater. Sci. Eng. C,* 2009, **29,** 2478-2485.

[3] D. P. Lew and F. A. Waldvogel, *Lancet,* 2004, **364,** 369-379.

[4] D. C. Hooper, *Biochim. Biophys. Acta.,* 1998, **1400,** 45-61.

[5] G. Cierny, J. T. Mader and J. J. Penninck, *Clin. Orthop.,* 2003, **414,** 7-24.

[6] H. Alvarez, C. Castro, L. Moujir, A. Perera, A. Delgado, I. Soriano, C. Evora and E. Sanchez, *J. Biomed. Mater. Res. B: Appl. Biomater.,* 2008, **85,** 93-104.

[7] M. Zilberman and J. J. Elsner, *J. Control. Release.,* 2008, **130,** 202-215.

[8] V. Mourino and A. R. Boccaccini, *J. R. Soc. Interface.,* 2010, **7,** 209-227.

[9] J. S. Price, A. F. Tencer, D. M. Arm and G. A. Bohach, *J. Biomed. Mater. Res.,* 1996, **30,** 281-286.

[10] B. V. Somayaji, U. Jariwala, P. Jayachandran, K. Vidyalakshmi and R. V. Dudhani, *J. Periodontol.,* 1998, **69,** 409-413.

[11] M. Ginebra, T. Traykova and J. A. Planell, *Biomaterials,* 2006, **27,** 2171-2177.

[12] L. Fan, J. Zhang and A. Wang, *J. Mater. Chem. B*, 2013, **1**, 6261-6270.

[13] R. V. Suganthi, K. Elayaraja, M. I. A. Joshy, V. S. Chandra, E. K. Girija and S. N. Kalkura, *Mater. Sci. Eng. C,* 2011, **31,** 593-599.

[14] M. Vallet-Regi and J. M. Gonzalez-Calbet, *Prog. Solid. State. Chem.,* 2004, **32,** 1-31.

[15] R. Freitag and F. Hilbrig, *Biotechnol. J.,* 2012, **7,** 90-102.

[16] Y. Kato, K. Nakamura and T. Hashimoto, *J. Chromatogr. A*, 1987, **398,** 340-346.

[17] M. Hong, J. Son, K. Kim, M. Han, D. S. Oh and Y. Lee, *J. Mater. Sci.: Mater. Med.,* **22,** 2011, 349-355.

[18] R. Murugan and S. Ramakrishna, *J. Mater. Sci.,* 2006, **41,** 4343-4347.

[19] G. S. Kumar and E. K. Girija, *Ceram. Inter.,* 2013, **39,** 8293-8299.

[20] Y. Yang, C. Liu, Y. Liang, F. Lin and K.C.-W. Wu*, J. Mater. Chem. B*, 2013, **1**, 2447-2450.

[21] R. Vani, S. B. Raja, T. S. Sridevi, K. Savithri, S. N. Devaraj, E. K. Girija, A. Thamizhavel and S. N. Kalkura, *Nanotech*., 2011, **22,** 285701.

[22] M. I. A. Joshy, K. Elayaraja, R. V. Suganthi, S. C. Veerla and S. N. Kalkura, *Curr. Appl. Phy.,* 2011, **11,** 1100-1106.

[23] C. Faucheux, E. Verron, A. Soueidan, S. Josse, M. D. Arshad, P. Janvier, P. Pilet, J. M. Bouler, B. Bujoli and J. Guicheux, *J. Biomed. Mater. Res. A,* 2009, **89,** 46-56.

[24] C. W. Kim, Y. Yun, H. J. Lee, Y. Hwang, I. K. Kwon and S. C. Lee, *J. Control. Release.,* 2010, **147,** 45-53.

[25] S. Dasgupta, S. S. Banerjee, A. Bandyopadhyay and S. Bose, *Langmuir,* 2010, **26,** 4958-4964.

[26] Q. Tang, Y. hu, J. Wu, F. Chen and S. Cao, *Nanomed.: Nanotechnol. Biol. Med.,* 2011, **7,** 428-434.

[27] G. D. Venkatasubbu, S. Ramasamy, V. Ramakrishnan and J. Kumar, *3 Biotech,* 2011, **1,** 173-186.

[28] C. Castro, E. Sánchez, A. Delgado, I. Soriano, P. Núñez, M. Baro, A. Perera and C. Évora, *J. Control. Release,* 2003, **93,** 341-354.

[29] C. Castro, C. Évora, M. Baro, I. Soriano and E, Sánchez, *Eur. J. Pharm. Biopharm.,* 2005, **60,** 401-406.

[30] A. L. Patterson, *Phys. Rev.,* 1939, **56,** 978-982.

[31] E. Landi, A. Tampieri, G. Celotti and S. Sprio, *J. Eur. Ceram. Soc.,* 2000, **20,** 2377-2387.

[32] A. C. Tas, *Biomaterials,* 2000, **21,** 1429-1438.

[33] http://www.iso.org/iso/home.htm.

[34] S. Koutsopoulos, *J. Biomed. Mater. Res.,* 2002, **62,** 600-612.

[35] C. Ergun, *J. Eur. Ceram. Soc*., 2008, **28,** 2137-2149.

[36] G. S. Kumar, E. K. Girija, A. Thamizhavel, Y. Yokogawa and S. N. Kalkura, *J. Colloid. Interface. Sci.,* 2010, **349,** 56-62.

[37] I. Turel, P. Bukovec and M. Quirds, *Inter. J. Pharm.,* 1997, **152,** 59-65.

[38] C. Gu and K. G. Karthikeyan, *Environ. Sci. Technol.,* 2005, **39,** 9166-9173.

[39] P. Trivedi and D. Vasudevan, *Environ. Sci. Technol.,* 2007, **41,** 3153-3158.

[40] http://www.chem.ucla.edu/~webspectra/irtable.html.

[41] K. Nakamoto, Infrared and Raman Spectra of Inorganic and Coordination Compounds Part B: Applications in Coordination, Organometallic and Bioinorganic Chemistry, John Wiley & Sons, New York, 2009.

[42] P. Venkatesan, N. Puvvada, R. Dash, B. N. P. Kumar, D. Sarkar, B. Azab, A. Pathak, S. C. Kundu, P. B. Fisher and M. Mandal, *Biomaterials,* 2011, **32,** 3794-3806.

[43] A. A. Silva-Junior, M. V. Scarpa, K. C. Pestana, L. P. Mercuri, J. Rosario de Matos and A. Gomes de Oliveira, *Thermochim. Acta,* 2008, **467,** 91-98.

[44] O. A. Ivashchenko, A. O. Perekos, N. V. Ulianchych, I. V. Uvarova, L. S. Protsenko, O. M. Budylina, M. Y. Holovkova and T. M. Yarmola, *Mat.-wiss.u.Werkstofftech.,* **42,** 2011, 98-108.

[45] T. Higuchi, *J. Pharm. Sci.* **52**, 1963, 1145-1149.

[46] F. Chen, P. Huang, Y. Zhu, J. Wu, C. Zhang and D. Cui, *Biomaterials*, **32**, 2011,9031-9039.

[47] P. L. Ritger and N. A. Peppas, *J. Control. Release.,* **5**, 1987, 23-36.

[48] P. L. Ritger and N. A. Peppas, *J. Control. Release.,* **5**, 1987, 37-42.

[49] G.K. Malik, I. Singh, S. Arora and V. Rana, *J. Adv. Pharm. Technol. Res.,* **2**, 2011, 163-169.

[50] M.H. Alkhraisat, C. Rueda, J. Cabrejos-Azama, J. Lucas-Aparicio, F.T. Mariño, J.T. García-Denche, L.B. Jerez, U. Gbureck and E.L. Cabarcos, *Acta Biomater*., **6**, 2010, 1522-1528.

[51] M. Ginebra, C. Canal, M. Espanol, D. Pastorino and E. B. Montufar, *Adv. Drug Deliv. Rev.,* 2012, **64,** 1090-1110.

[52] K. Drlica and X. Zhao, *Microbiol. Mol. Biol. Rev.*, 1997, **61,** 377-392.

[53] D. C. Hooper, *Drugs,* 1999, **58,** 6-10.

[54] M. Vallet-Regi and D. Arcos, *J. Mater. Chem.,* 2005, **15**, 1509-1516.

Tables

Table. 1. Average crystallite size and degree of crystallinity of the as-synthesized samples

Sample code	Concentration of ciprofloxacin (mg/ml)	Average crystallite size (nm)	Degree of crystallinity
Pure HA	0	40 ± 02	1.646
HA-cip-1	5	39 ± 04	1.537
HA-cip-2	10	37 ± 03	1.309
HA-cip-3	20	31 ± 02	0.764

Table. 2. The kinetic parameters of experimental drug release data fitted with Higuchi and Ritger-Peppas model.

Sample code	Higuchi model	Ritger-Peppas model	
	Correlation coefficient (r^2)	Correlation coefficient (r^2)	Diffusional exponent (n)
HA-cip-1	0.94	0.99	0.60
HA-cip-2	0.98	0.98	0.57
HA-cip-3	0.99	0.98	0.56

Table. 3. Zone of inhibition of as-synthesized samples against *E. coli* and *S. aureus*

Sample code	Diameter of zone of inhibition (cm)	
	E. coli	*S. aureus*
HA	0	0
HA-cip-1	3.5 ± 0.2	3.5 ± 0.2
HA-cip-2	3.7 ± 0.2	3.8 ± 0.3
HA-cip-3	3.9 ± 0.2	3.8 ± 0.2

Figures

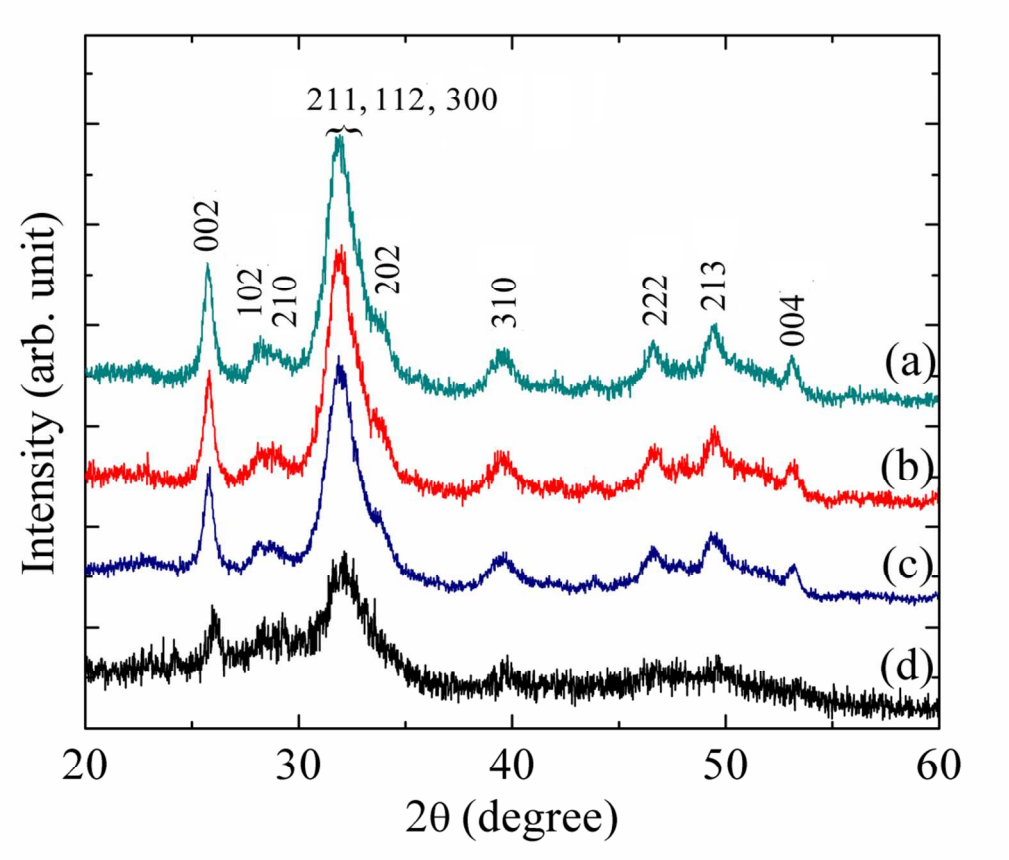

Fig. 1. PXRD patterns of samples (a) pure HA, (b) HA-cip-1, (c) HA-cip-2 and (d) HA-cip-3.

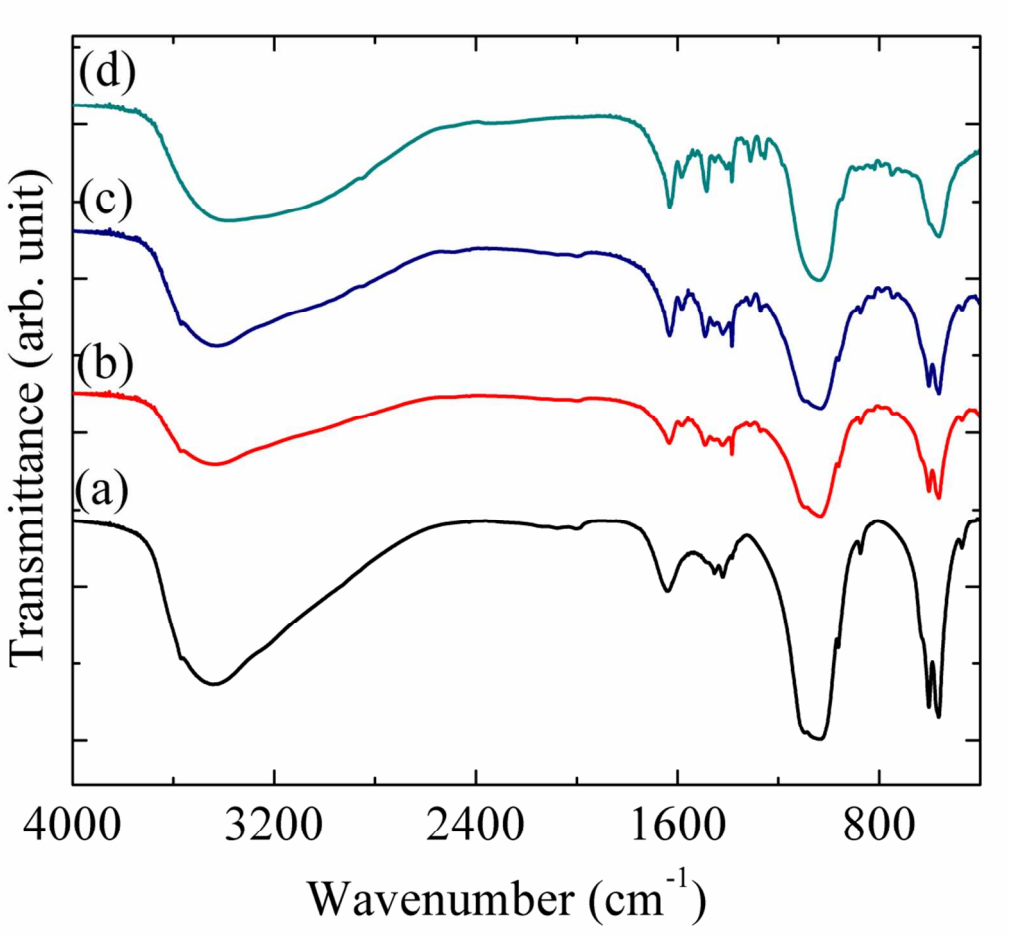

Fig. 2. FT-IR spectra of samples (a) pure HA, (b) HA-cip-1, (c) HA-cip-2 and (d) HA-cip-3.

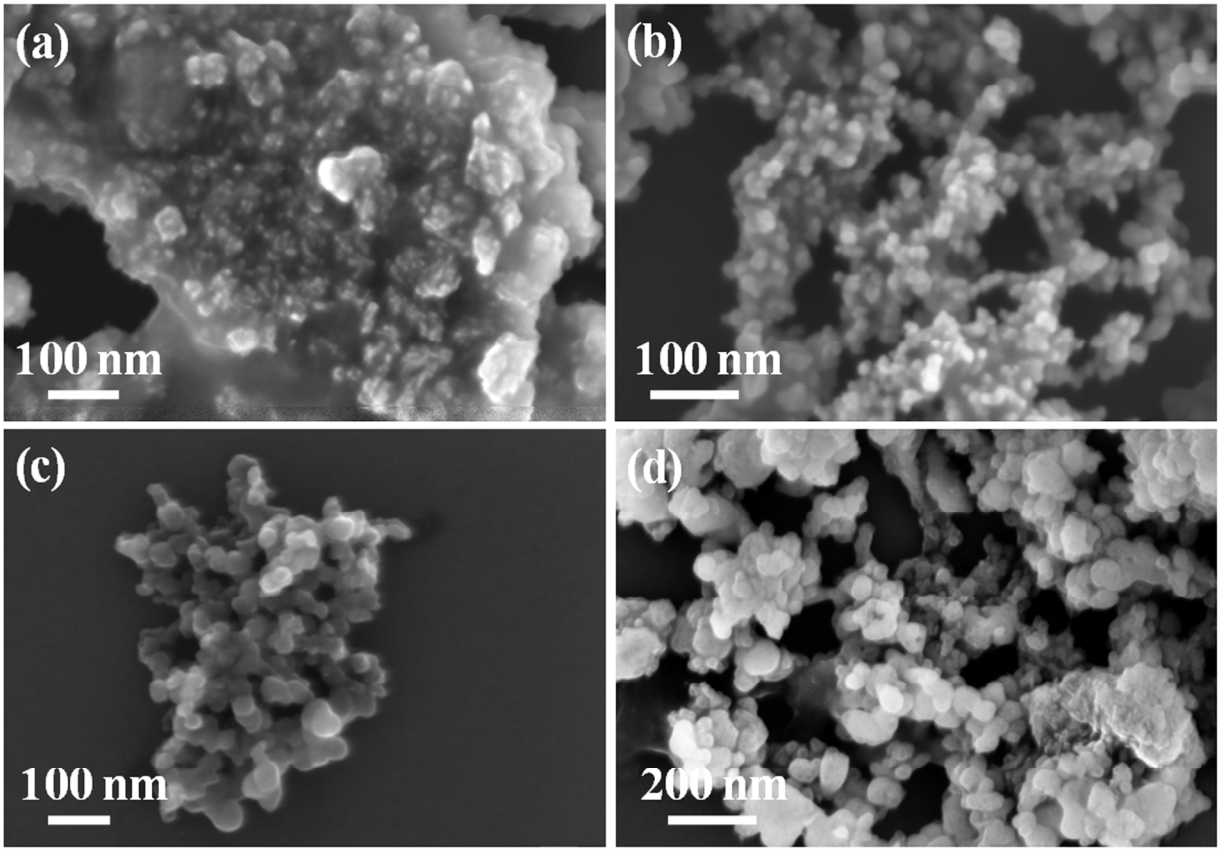

Fig. 3. FESEM image of samples (a) pure HA, (b) HA-cip-1, (c) HA-cip-2 and (d) HA-cip-3.

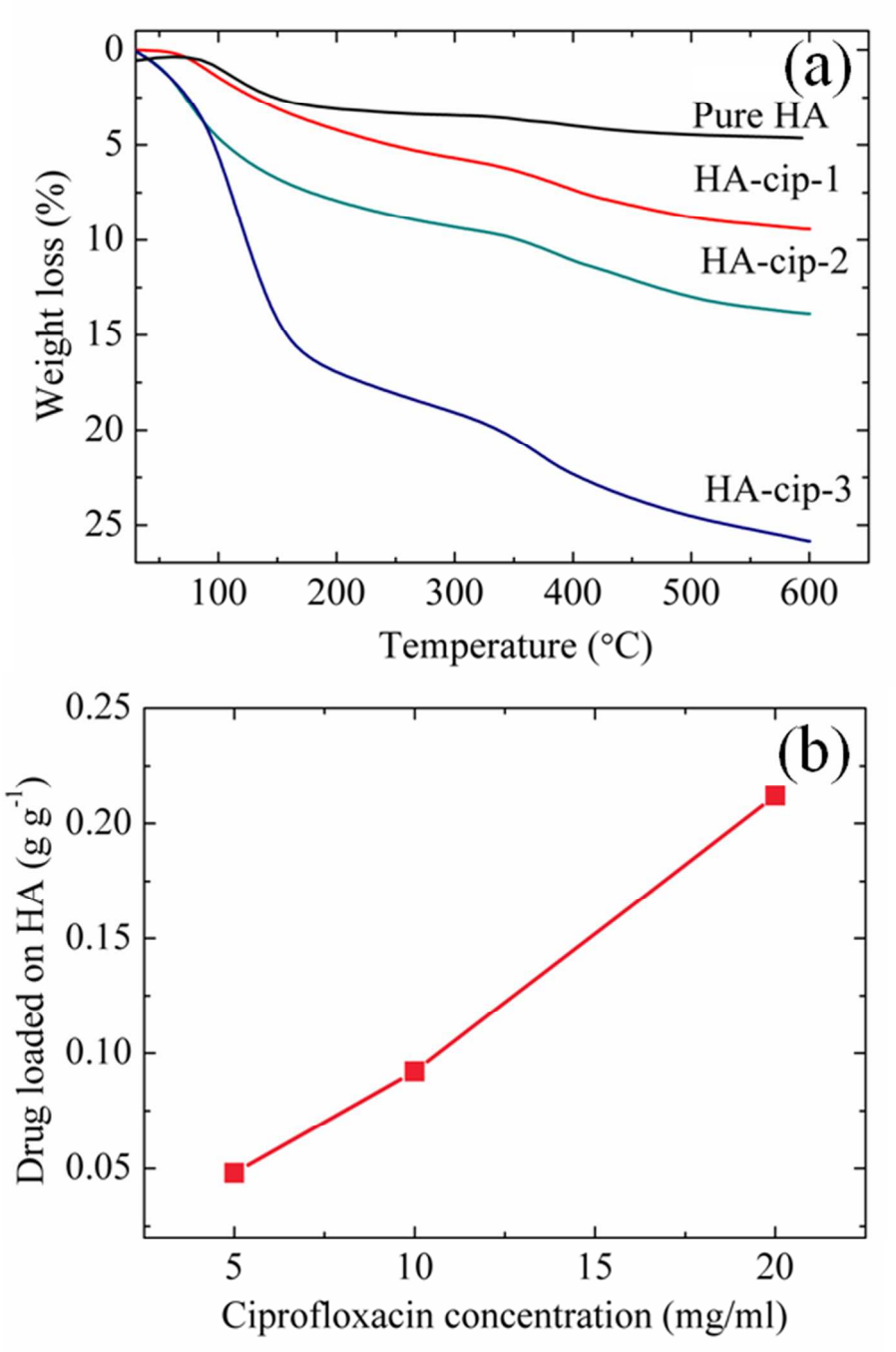

Fig. 4. (a) TG curve of as-synthesized samples and (b) initial concentration of ciprofloxacin during the synthesis of HA versus amount of drug loaded on HA.

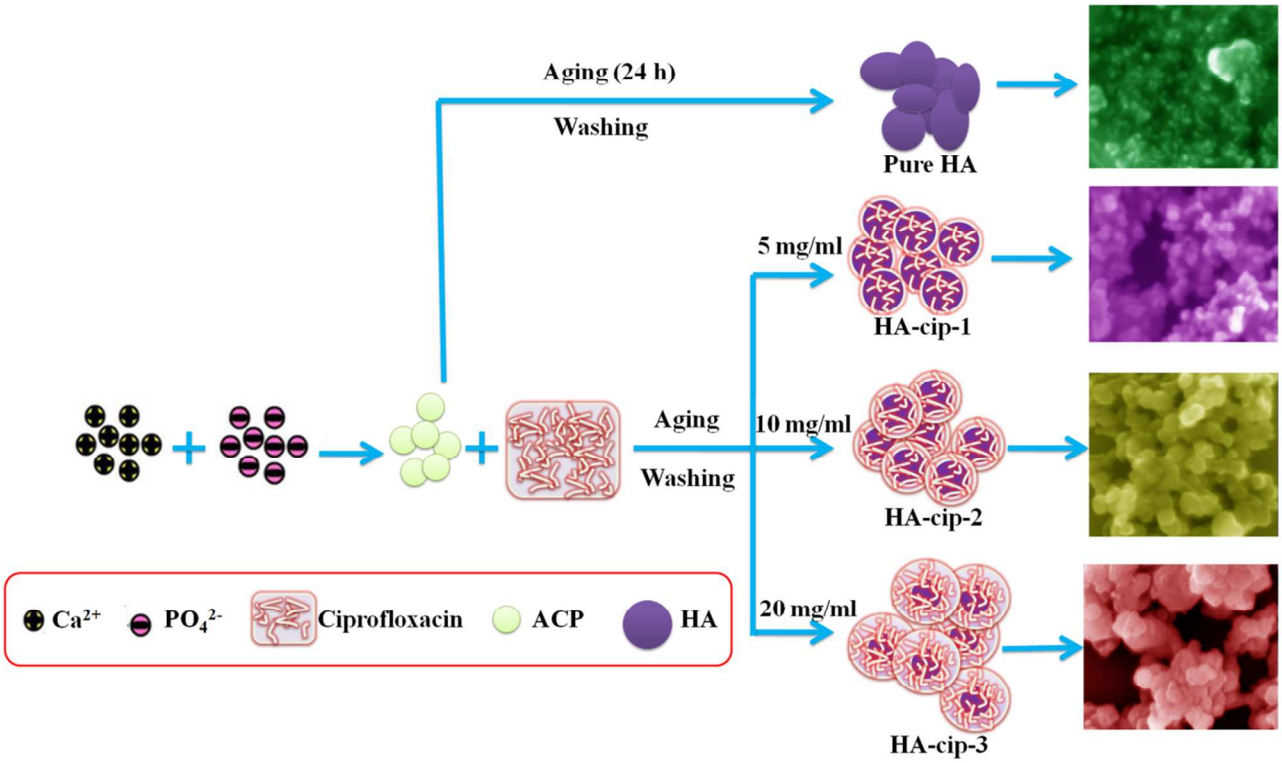

Fig. 5. Schematic of *in situ* formation of ciprofloxacin loaded HA nanoparticles.

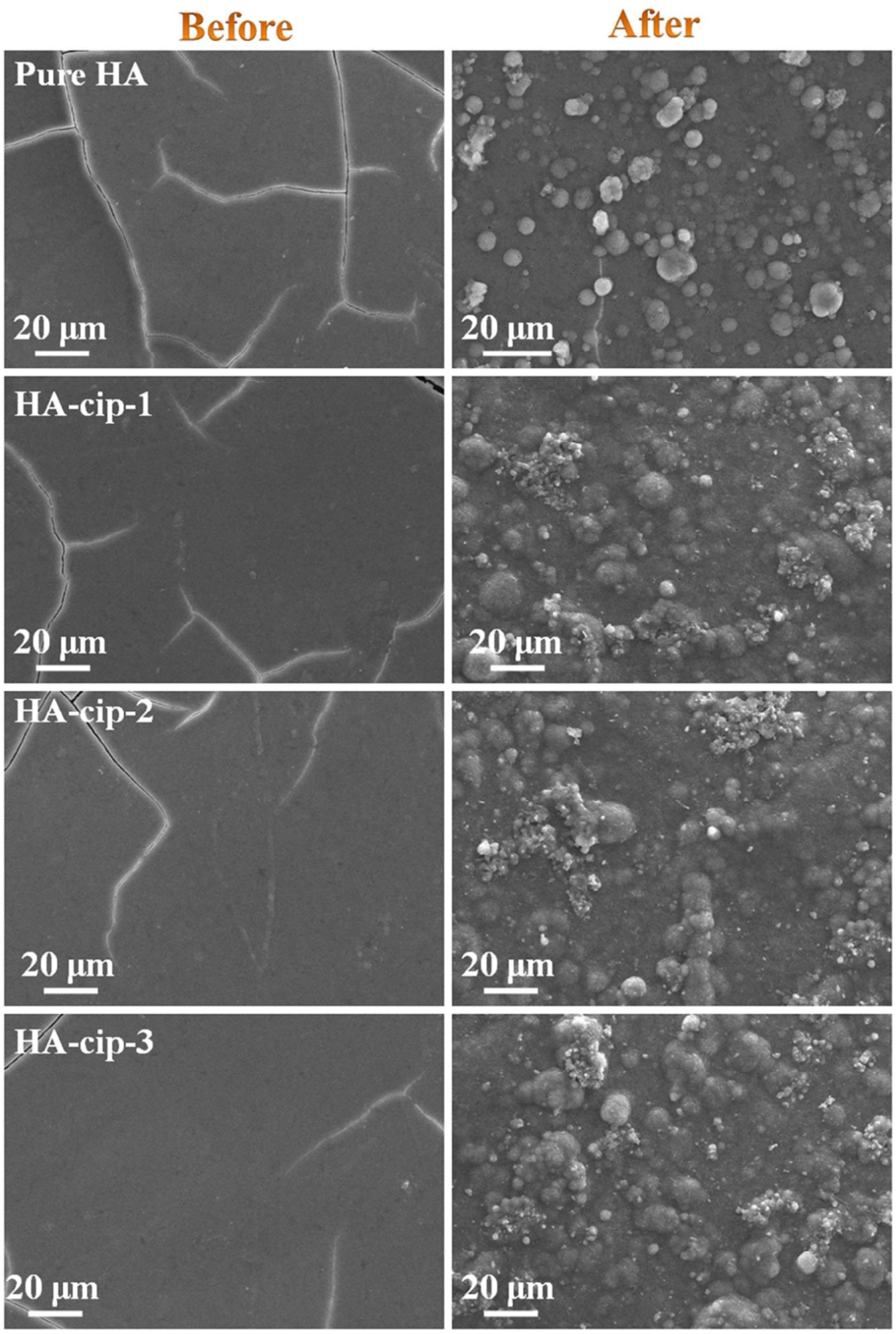

Fig. 6. SEM images of the surface of compacted samples before and after soaking in SBF for 21 days.

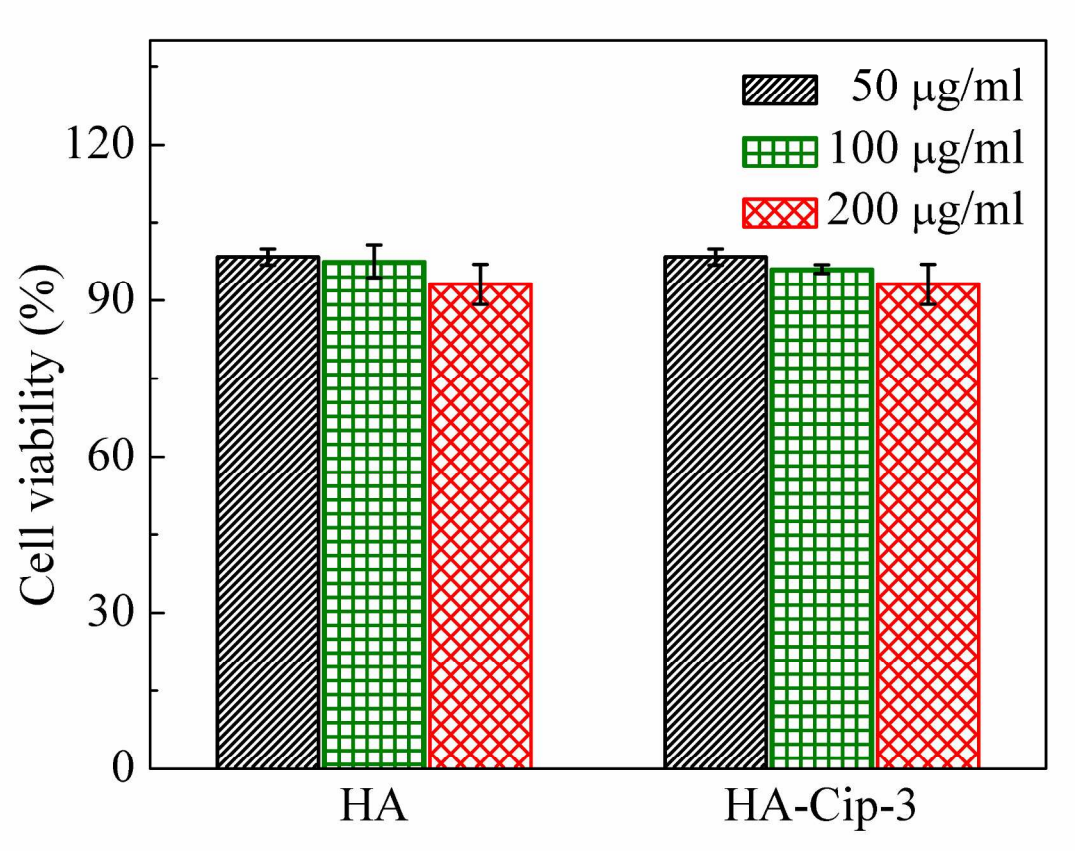

Fig. 7. Cell viability of HA and HA-cip-3 with human osteoblast MG-63 cells.

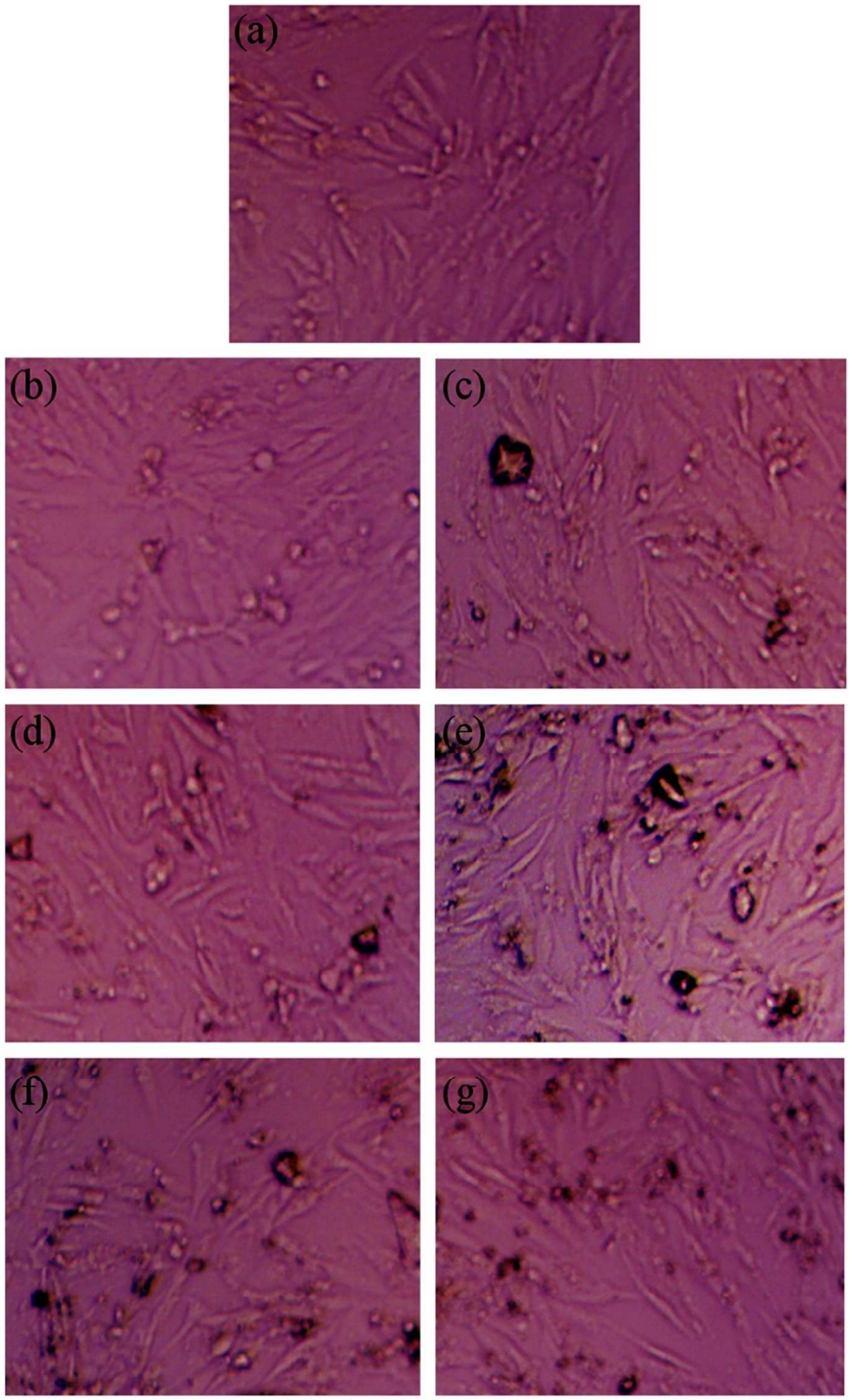

Fig. 8. Optical image of human osteoblast like MG-63 cells and cells cultured with different dosages of samples (a) Control, (b) 50 μg/ml of HA, (c) 100 μg/ml of HA, (d) 200 μg/ml of HA, (e) 50 μg/ml of HA-cip-3, (f) 100 μg/ml of HA-cip-3, (g) 200 μg/ml of HA-cip-3, after 48h incubation.

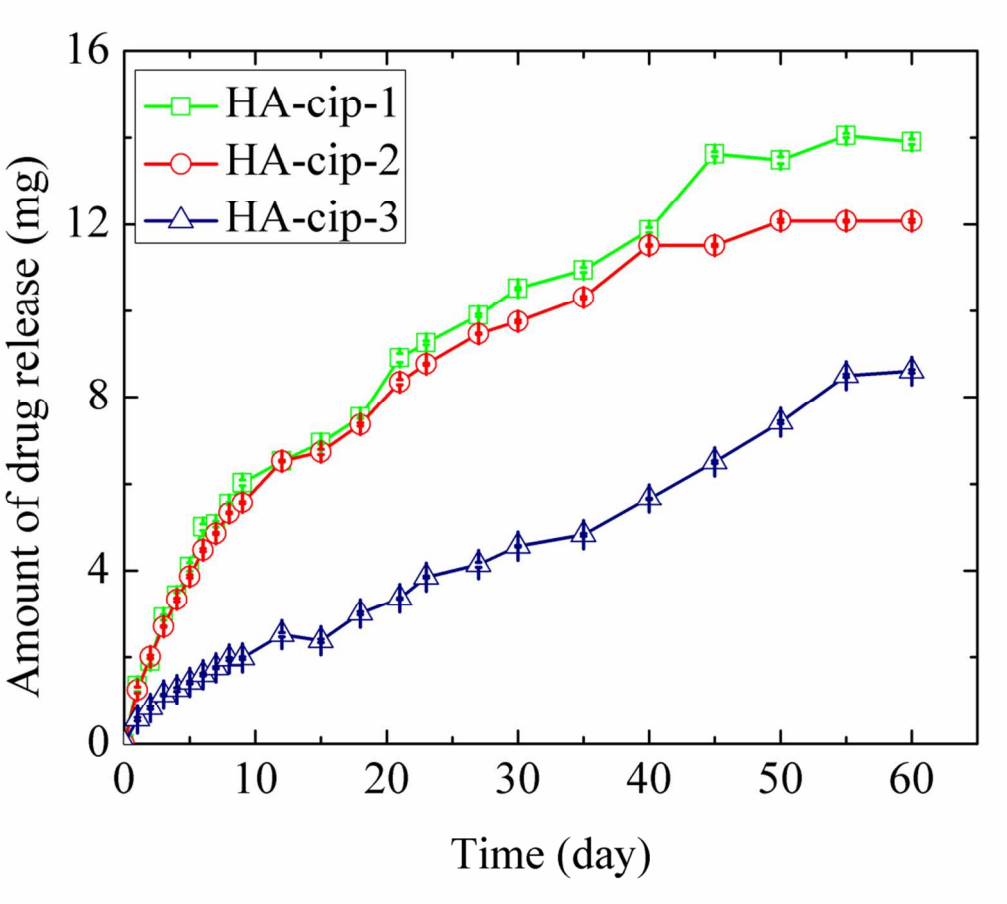

Fig. 9. Plot between amount of ciprofloxacin released from the *in situ* prepared ciprofloxacin loaded HA nanoparticles and time.

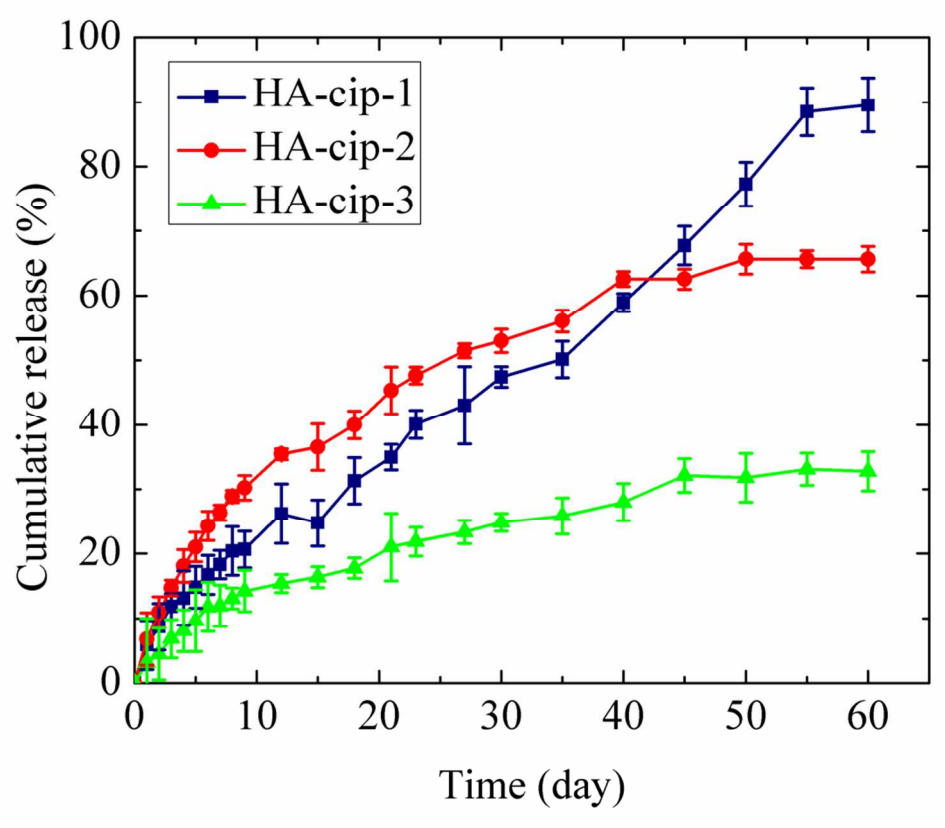

Fig. 10. Plot of cumulative release of ciprofloxacin from the *in situ* prepared ciprofloxacin loaded HA nanoparticles as a function of time.

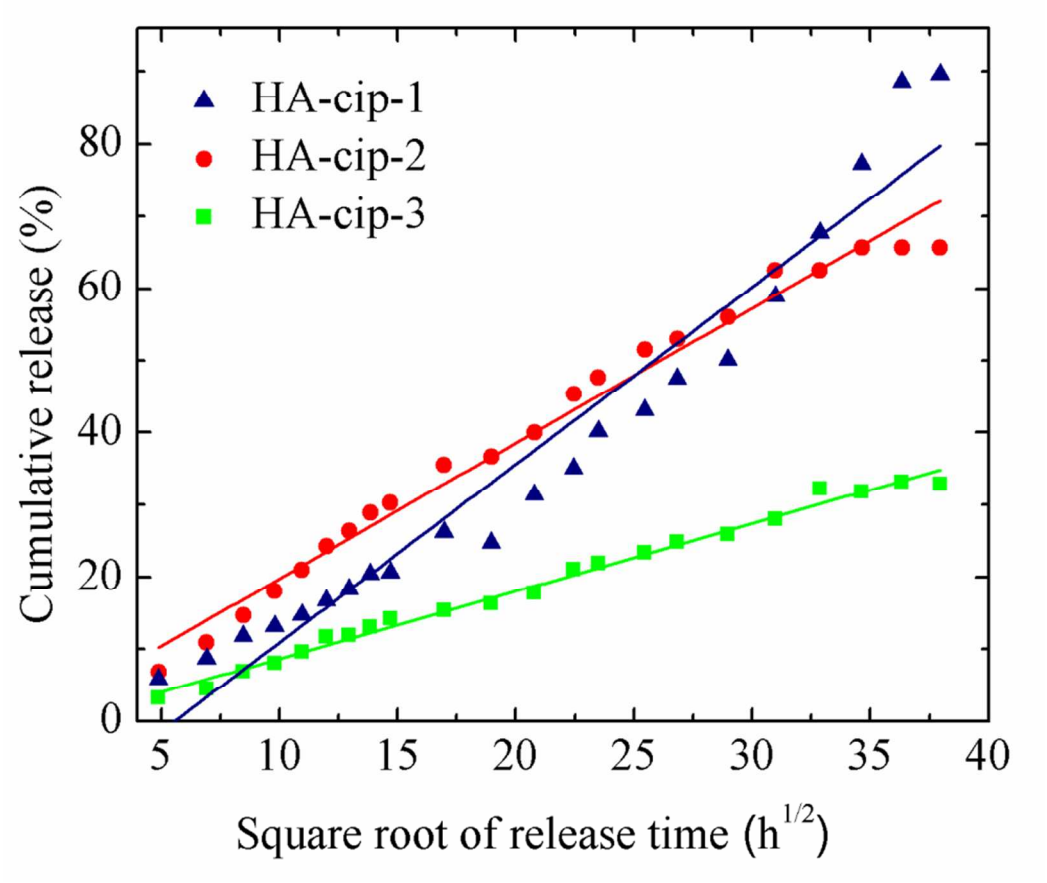

Fig. 11. Plot of cumulative drug release percentage versus square root of release time for HA-cip-1, HA-cip-2 and HA-cip-3. Solid lines represent data fitting to the Higuchi model.

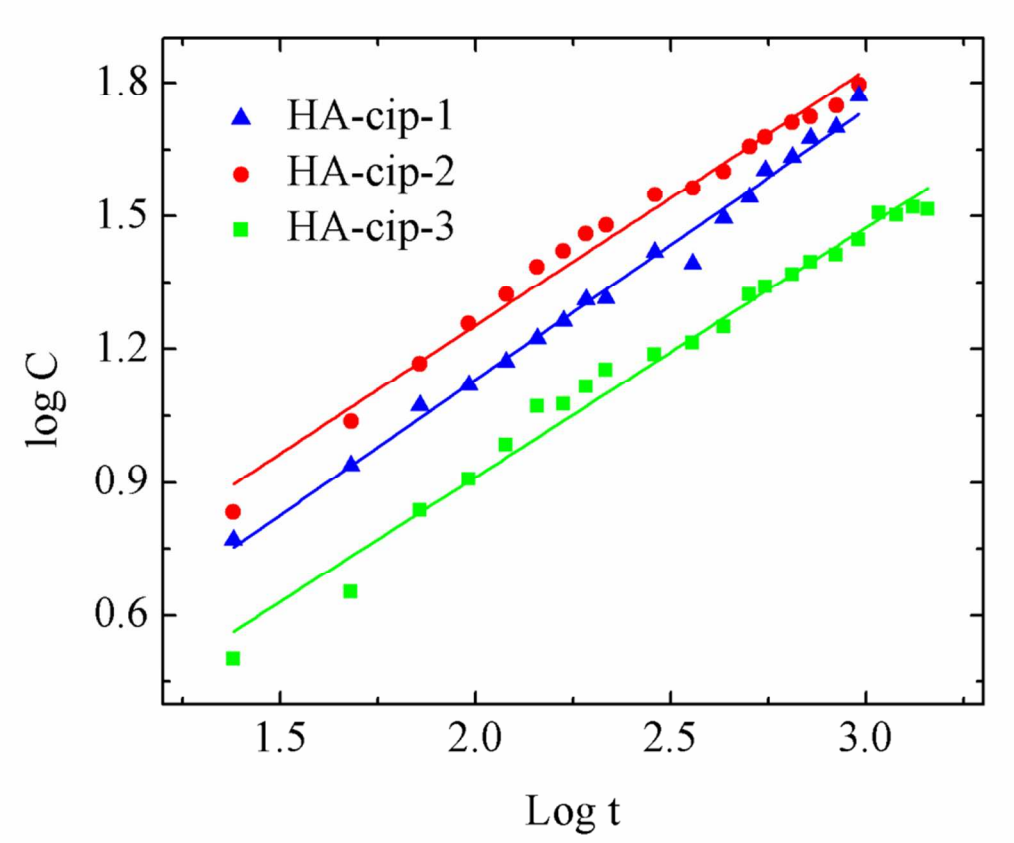

Fig. 12. Plot of log cumulative drug release percentage as a function of log time for HA-cip-1, HA-cip-2 and HA-cip-3. Solid lines represent data fitting to the Ritger-Peppas model.

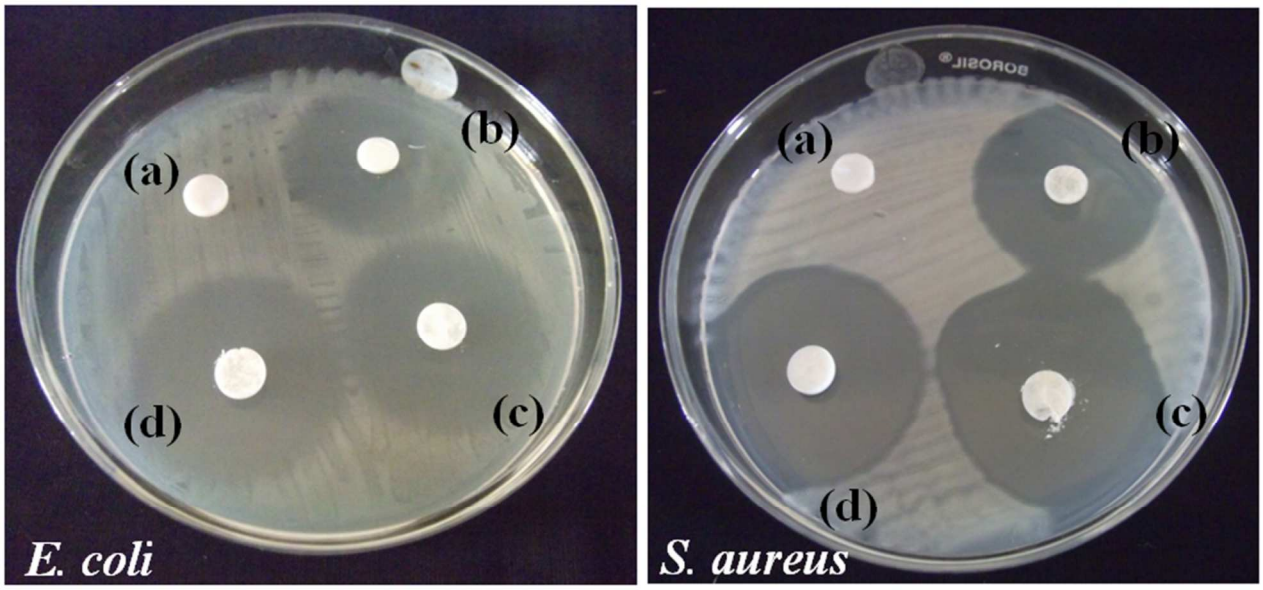

Fig. 13. Inhibition zone formed around the samples disks against *E. coli* and *S. aureus* cultures (a) pure HA, (b) HA-cip-1, (c) HA-cip-2 and (d) HA-cip-3.

Graphical abstract

A series of ciprofloxacin loaded hydroxyapatite nanoparticles has been synthesized by *in situ* precipitation method for osteomyelitis treatment.